Coordination Chemistry Reviews 256 (2012) 2521–2529

Contents lists available at SciVerse ScienceDirect

Coordination Chemistry Reviews

journal homepage: www.elsevier.com/locate/ccr

Review

Toward solar fuels: Water splitting with sunlight and "rust"?

Michael J. Katz[a,b], Shannon C. Riha[a,d], Nak Cheon Jeong[a,b], Alex B.F. Martinson[a,d], Omar K. Farha[a,b], Joseph T. Hupp[a,b,c,d,*]

[a] Argonne-Northwestern Solar Energy Research (ANSER) Center, Northwestern University, 2145 Sheridan Road, Evanston, IL 60208, USA
[b] Dept. of Chemistry, Northwestern University, 2145 Sheridan Road, Evanston, IL 60208, USA
[c] Chemical Science and Engineering Division, Argonne National Laboratory, Argonne, IL 60439, USA
[d] Materials Science Division, Argonne National Laboratory, Argonne, IL 60439, USA

Contents

ARTICLE INFO

Article history:
Received 30 March 2012
Received in revised form 18 June 2012
Accepted 19 June 2012
Available online 27 June 2012

Keywords:
Hematite
Solar fuels
Alternative energy

ABSTRACT

Iron(III)oxide in the form of hematite is, in many respects, an attractive material for the photocatalytic production of molecular oxygen from water. Especially over the past six years, several developments have advanced the performance of water oxidation cells based on this material. Nevertheless, the best versions of these photoelectrodes produce only about a fifth of the maximum photocurrent (and dioxygen) theoretically obtainable, while operating at photovoltages also well short of the theoretical maximum. Here we describe the factors limiting the performance of hematite as a photo-catalyst and outline approaches that have been, or might be, tried to overcome them. These factors include low hole mobility, bulk charge recombination, surface charge recombination, slow water oxidation kinetics, and poor light absorption. Whether hematite will soon become a practical photo-catalyst for water oxidation is uncertain. But, the schemes developed and the lessons learned will likely prove transferrable to other candidate photocatalyst materials.

1. Introduction

Water is a ubiquitous, and mostly untapped, source for the ultimate cleaning-burning fuel, molecular hydrogen. Since the product of hydrogen combustion is water, it also is a renewable source. Likewise, if used in a fuel cell to generate electricity, the ultimate product from H_2 oxidation is water. Fuel-cell based consumption of H_2 is attractive, in part, because it circumvents the efficiency limitations imposed by the Carnot cycle on heat engines.

The minimum energy required at room temperature to transform two moles of water into one mole of molecular oxygen and two moles of molecular hydrogen is ca. 475 kJ. Writing the water splitting reaction (Eq. (1c)) in terms of component half reactions (Eqs. (1a) and (1b)), it is clear that oxidation of two water molecules to one molecule of O_2 requires four holes (or equivalently, produces

* Corresponding author at: Argonne-Northwestern Solar Energy Research (ANSER) Center, Northwestern University, 2145 Sheridan Road, Evanston, IL 60208, USA.
E-mail address: j-hupp@northwestern.edu (J.T. Hupp).

0010-8545/$ – see front matter © 2012 Elsevier B.V. All rights reserved.
http://dx.doi.org/10.1016/j.ccr.2012.06.017

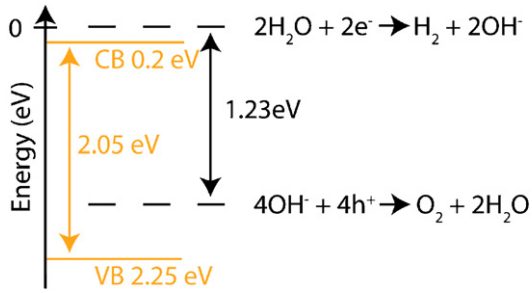

Fig. 1. Energy diagram showing potentials for aqueous hydrogen and oxygen evolution reactions, and the conduction band (CB) and valence band (VB) edge of hematite, versus the normal hydrogen electrode (NHE). Note that the sign convention for electrochemical potentials is the reverse of that for absolute energies versus vacuum (i.e. an energy of zero for an electron in vacuum). Thus, electrochemical potentials become more positive as one moves downward along the energy axis, while absolute energies become more negative.

four electrons), while reduction of two protons to one molecule of H_2 consumes two electrons:

$$2\,[2H^+ + 2e^- \rightarrow H_2] \tag{1a}$$

$$2H_2O + 4\,h^+ \rightarrow O_2 + 4H^+ \tag{1b}$$

$$2H_2O \rightarrow 2H_2 + O_2 \tag{1c}$$

At high pH the half reactions are:

$$2\,[H_2O + 2e^- \rightarrow H_2 + 2OH^-] \tag{2a}$$

$$4OH^- + 4\,h^+ \rightarrow O_2 + 2H_2O \tag{2b}$$

[In the above equations and in Fig. 1, h^+ denotes a hole.]

In the absence of special effects like singlet–triplet fission, one photon, when absorbed by a molecule, molecular aggregate, molecular solid, or non-molecular solid can produce, at most, one electron/hole pair. It follows that solar-driven water splitting via redox reactions requires four photons, with a minimum average energy of 1.23 eV (or ca. 119 kJ per mol of photons). The corresponding optical wavelength is ca. 1008 nm, i.e. well into the near-infrared region.

Realistically, even for highly catalytic molecules or materials, significant additional energy is needed to drive the splitting reactions at reasonable rates. Assuming no losses other than kinetic overpotentials (of, say, 0.4 V for oxidation and 0.2 V for reduction), four photons of average energy 1.83 eV would be needed to split a pair of water molecules into H_2 and O_2. The corresponding optical wavelength is 678 nm, i.e. near the red limit of the visible spectrum.

The good news is that many molecules absorb and transiently store visible-region photonic energy at levels above 1.83 eV. Likewise, many semiconductors feature electronic band gaps above 1.83 eV, but still absorb light across a substantial fraction of the visible spectrum. One of the most intriguing photocatalytic semiconductors is crystalline Fe_2O_3 in the form of hematite [1–3]. Constituting the most common form of iron ore, hematite is plentiful and inexpensive. Depending on how it has been processed (e.g. polished), hematite can vary in color from rust red to nearly black. While it can be found on steel surfaces where it constitutes a rust-like corrosion product, strictly speaking it differs from rust, which consists of any of several *hydrated* forms of iron(III)oxide.

Hematite (α-Fe_2O_3) offers a bandgap of ~2.05 eV, corresponding to an absorption onset wavelength of ~605 nm. The higher the bandgap, the greater will be the driving force available for one or both of the water-splitting half reactions and the more likely the reaction(s) will proceed at an acceptable rate. A larger bandgap, of course, also means that a smaller fraction of the solar spectrum can be captured and fewer photo-excited electron/hole pairs can be generated. Based on the terrestrial solar spectrum at 1 sun, and the absorption onset for α-Fe_2O_3, the upper limit for the photocurrent density of hematite is ca. 13 mA/cm^2. Hematite also offers excellent chemical and morphological stability, at least under neutral and basic conditions. Additionally, it is easily doped, can be synthesized in any of several ways, in any of several microscopic morphologies, and on a broad range of support surfaces.

Despite these attractive characteristics, α-Fe_2O_3 is not yet an effective material for photocatalytic conversion of water to solar fuel. Nevertheless, there has been considerable recent research aimed at understanding why hematite is not a champion photocatalytic material or aimed at modifying or adding to its properties so as to make it photocatalytically efficacious. Below the challenges/difficulties with α-Fe_2O_3 as a photocatalyst are outlined. Then, work directed toward understanding and/or overcoming these challenges is critically reviewed. The emphasis is on recent developments and the work covered is representative, rather than comprehensive. For more detailed or comprehensive discussions, any of several recent reviews or perspective articles can be consulted [4–11].

2. Challenges

While the band gap of hematite is great enough to enable selective absorption of photons having sufficient energy to drive water-splitting reactions, its band edges are not optimally positioned. In particular, the conduction-band edge of α-Fe_2O_3 falls a few hundred millivolts short of what is needed thermodynamically to drive the reduction of water to molecular hydrogen. The valence band edge, in contrast, is positioned several hundred millivolts positive of the thermodynamic potential for oxygen evolution. Thus, in order to split water completely it is necessary to couple hematite illumination with illumination of a secondary photoelectrode. Fortunately, a significant fraction of the photons remaining after absorption of blue and green light by hematite are, in principle, energetic enough to make up the shortfall by hematite and drive the coupled water reduction reaction.

A second problem is that hematite is a weak absorber, especially at longer wavelengths. Indeed, at the red-most wavelengths that incite photo-activity, the optical depth (90% light-absorption depth) is around 600 nm. Unfortunately, the distance that photogenerated holes can travel before recombining with electrons is only about 4–10 nm (where the precise value is likely dependent on the extent of semiconductor doping) [4,7,12–14,3,15–17]. The short transport length is a consequence of both the short lifetime of the photo-excited electron/hole pair (estimated to be a few ps) [18] and the low mobility of the hole. The practical consequence is that only those holes (oxidizing equivalents) that are generated within a few to several nanometers of the semiconductor/solution interface can reach the interface and be used for water or hydroxide ion oxidation, with the rest recombining with electrons and generating only heat (Fig. 2).

Closely related to short hole-transport distances and rapid recombination of holes and electrons within the semiconductor is surface-defect-catalyzed carrier recombination [19–22]. Obviously, any holes suffering surface-catalyzed recombination are unable to contribute to photochemical oxygen production.

A fourth problem is the comparatively low reactivity of holes (manifest, in part, as slow electrochemical kinetics) once they reach the electrode/solution interface. Absorbed-photon-to-current-efficiency (APCE) values are wavelength dependent, ranging from as high as 0.49 for UV photons (λ = 300 nm) to 0.05 or less for photons near 600 nm; see Fig. 3 [17]. These low values may reflect, in part, low reactivity of holes with water molecules or hydroxide ions (although energy-dependent bulk recombination may also be a factor). The mechanism for photo-catalytic oxygen

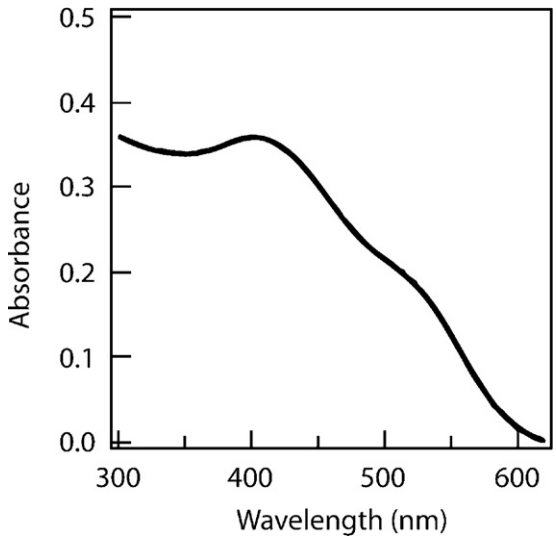

Fig. 2. Absorption spectrum of a 25 nm film of ALD-grown hematite. Reprinted with permission from [17]. Copyright 2011 American Chemical Society.

evolution on α-Fe_2O_3 is unknown. Nevertheless, there is compelling evidence from variable-temperature transient absorbance measurements that the rate-determining step involves a substantial activation energy that is independent of applied potential [12,22].

A fifth issue is poor conductivity, especially with thicker photoelectrodes. Collectively these issues have limited photocurrents to only about a quarter of the theoretical maximum value (and, more typically, about 5%) and photo-catalysis onset potentials to several hundred millivolts positive of the most favorable potentials achievable theoretically.

3. Progress toward solutions

3.1. Materials synthesis

Amorphous iron oxide is easily prepared and subsequent conversion to crystalline α-Fe_2O_3 can typically be accomplished via heating to ca. 500 °C. Desirable for photoelectrochemical applications, however, are syntheses that can be accomplished on transparent conductive platforms and that yield comparatively

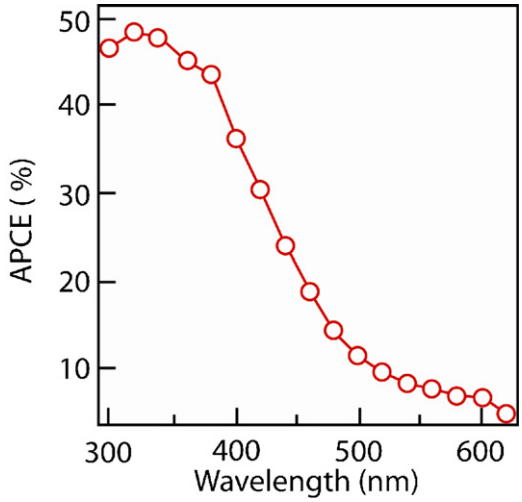

Fig. 3. Absorbed photon-to-current efficiency of planar Fe_2O_3. Reprinted with permission from [17]. Copyright 2011 American Chemical Society.

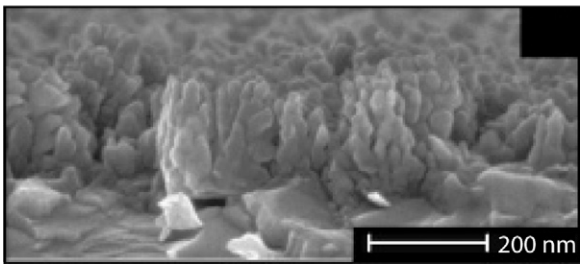

Fig. 4. Side-view of Si(IV)-doped hematite as grown by APCVD. Reprinted with permission from [29]. Copyright 2006 American Chemical Society.

high surface area structures, textured on length scales not too different from distances that holes can move. These features facilitate the delivery of oxidizing equivalents to the hematite/solution interface. Also desirable is the ability to dope hematite structures with ions of metals or semi-metals, so as to manipulate conductivity. Usually preferred are dopants in oxidation state (IV), as these generally yield n-type hematite—which will tend spontaneously (because of band bending) to move photo-generated holes to the electrode/solution interface and electrons toward the electrode interior (and, eventually, to an underlying or encapsulated current collector). Occasionally preferred is p-type hematite, in combination with n-type [23]. Metal ion dopants in oxidation state (II) are effective for obtaining hematite in p-type form. (In the absence of intentional doping, hematite is generally n-type—a consequence of oxygen deficiency.)

Among the many approaches that have been explored for hematite synthesis are magnetron sputtering [24], electrochemical deposition [25], ultrasonic spray pyrolysis [26], solution saturation of precursor compounds [27], conventional chemical vapor deposition [2], and atmospheric-pressure chemical vapor deposition (APCVD) [28,29]. An important advance, described by Kay et al. in 2006, was the discovery that APCVD-based fabrication of Si(IV)-doped iron oxide on planar conductive-glass platforms could yield comparatively high area, textured hematite [28–30]. As shown in Fig. 4, the oxide takes the form of closely spaced blades or platelets oriented normal to the supporting platform. Notably, the orientation is such that the most highly conductive planes of the exceptionally anisotropic material are directed perpendicular to the current collector (i.e. supporting platform).

Finally, atomic layer deposition (ALD) has attracted attention as a means of fabricating hematite, with or without intentional doping [13,15,21,23,31]. The most compelling features of ALD methods are that they are conformal (as opposed to line-of-sight), they provide close to angstrom-level control over thickness, and they deposit material reproducibly and uniformly. ALD is especially useful for preparing smooth (non-scattering) and ultra-thin films of precise, pre-determined thickness, either on flat platforms (for fundamental studies) or on high-area platforms (for achieving high light collection). See Fig. 5 for examples.

3.2. Enhancing absorption cross sections

At longer wavelengths α-Fe_2O_3 behaves as an indirect semiconductor, so absorbs light weakly. A recent electronic structure study by Liao and Carter of embedded molecular cluster models provides some insight [32]. Consistent with earlier interpretations, cluster absorption at longer wavelengths is assigned to a Laporte-forbidden d–d transition (Fe-localized $t_{2g} \rightarrow e_g$). At considerably shorter wavelengths, the absorption is due mainly to allowed ligand-to-metal charge-transfer (LMCT) transitions (oxo-to-iron transitions), while at intermediate wavelengths absorption is attributed to partially allowed transitions having mixed LMCT

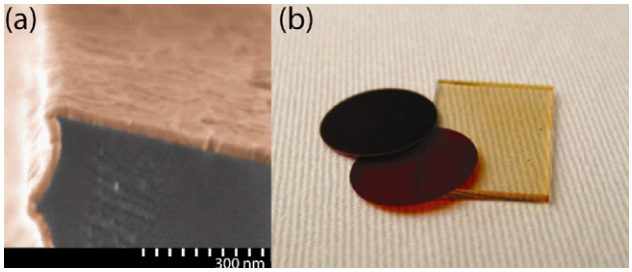

Fig. 5. (a) False color SEM micrograph of a hematite film deposited conformally by ALD on an irregular silicon substrate (hematite shown in false color). (b) 7 nm ALD-grown film of hematite on a square glass substrate, and 7 nm ALD-grown films of hematite on porous, transparent anodic-aluminum-oxide (AAO) membranes. The surface areas of the round and highly porous AAO membranes are hundreds (lower) or thousands (upper) of times greater surface area than geometric areas.

and d–d character. The authors state that accurate evaluation of these systems via most DFT methods is inherently error prone and argue that their application to hematite and associated model compounds generally should be avoided.

Given the symmetry-forbidden nature of the lowest-energy photo-active excitation, one possible strategy to increase absorption cross-sections would be to introduce ionic dopants that are either larger or smaller than Fe(III) [33,34]. The resulting lattice distortions might be expected to lower the ground-state symmetry sufficiently to make low-energy transitions more strongly allowed, thereby boosting light absorption. There are indications in the literature on metal-oxides as pigments that this approach might be effective [35]. Experimental work in that area, however, has focused mainly on highly scattering particulate forms of hematite. Consequently, inferences about modulation of absorption cross sections have largely come from reflectance rather than absorptance measurements. While these measurements seem to indicate that doping engenders significant (but not large) increases in absorption cross sections, our own experience with non-scattering hematite samples fabricated via atomic layer deposition is that the effects if present at all, are small. Souza et al. have reported similar findings; specifically, they report that hematite doping with Si(IV) increases absorption cross sections by only a few percent [36].

An alternative strategy for increasing the light harvesting efficiencies makes use of localized surface plasmon resonance. Nanoparticles of metals such as silver, copper, and gold feature intense visible-region plasmon absorption bands [37]. Plasmonic excitations cause coherent oscillations of vast numbers of free electrons. As a consequence, enormous short-range (a few to several nanometers) electromagnetic fields are generated. These fields are responsible for the million-fold and greater amplification effects that characterize surface-enhanced Raman scattering [38]. Less well recognized is that these fields can also enhance electronic absorption cross-sections of proximal molecules and materials—albeit, to much lesser extent than for Raman scattering [39]. Advantage of this effect has been taken to demonstrate photocurrent enhancements of up to seven-fold in dye-sensitized solar cells featuring only a monolayer of dye on a nominally flat semiconductor platform [40]. Also demonstrated was the expected sharp fall-off of amplification effects with separation distance between metal particles and dye molecules [40]. Subsequent work by Chen et al. has placed these findings on a firm theoretical footing [41,42]. (Extension of the experimental approach to conventional high-area dye-coated electrodes has also yielded photocurrent enhancements, but of a much smaller relative magnitude [43,44].)

Similar amplification behavior would be expected for materials—and a persuasive example involving gold nanoparticles

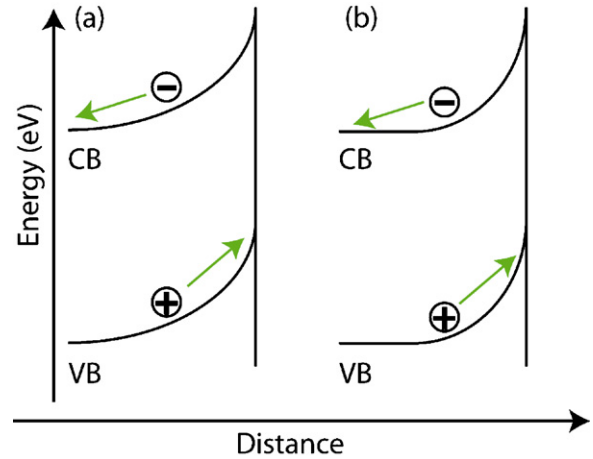

Fig. 6. (a) Space-charge layer of lightly doped n-type hematite; band bending separates the electron–hole pair such that the electron travels toward the interior, and the hole travels to the surface of the hematite film. (b) Space-charge layer of more heavily doped hematite film; doping decreases the space-charge layer thickness.

and hematite has been described by Thomann et al. [45]. They observed a 4-fold enhancement of the otherwise very weak absorbance by hematite around 600 nm. A challenge in capitalizing further on this approach will be to avoid large losses due to competitive light absorption by metal nanoparticles. Nevertheless, several preliminary reports have been published, and these have been critically reviewed by Warren and Thimsen [46].

3.3. Enhancing hole transport and slowing bulk recombination of holes and electrons

Recombination of photo-generated holes with electrons can occur both within the semiconductor and on its surface. In either case, it diverts oxidizing equivalents from photo-catalysis and, therefore, diminishes quantum yields and photocurrent production. For planar electrodes comprising hematite that has not been intentionally doped, anodic photocurrents are largest when the semiconductor thickness is 20–30 nm. Thinner electrodes obviously collect less light, so understandably deliver less photocurrent. For thicker electrodes, reports by Wang and co workers [17] and by Hamann and co workers [13] are instructive. Both teams have noted that photocurrents decrease once the thickness of the electrode exceeds the thickness of the space-charge layer (ca. 25 nm in the work by Wang et al. and ca. 17 nm in the work by Hamann et al.). The potential gradient associated with the space-charge layer should facilitate separation of holes and electrons, driving the former toward the electrode/solution interface and the latter toward the electrode interior and ultimately, toward a current collector; see Fig. 6a.

In view of the low current collection efficiencies for hematite photo-electrodes—as low as 0.05 at long wavelengths, and no greater than 0.49 at any wavelength (see Fig. 3)—it appears that the voltage gradient is only partially effective at facilitating charge separation. Doping with mono-atomic ions of charge greater than 3+ will introduce additional majority carriers (i.e. electrons) and create steeper voltage gradients (thinner space-charge layers). In turn, these should enhance charge separation. The trade-off would be a need to shift to even thinner electrodes for optimal charge collection (as only holes generated within the now narrower space-charge layer are likely to contribute to water oxidation); see Fig. 6b. Unfortunately, traditional approaches to formation of iron(III)oxide films yield amorphous material, even after thermal annealing, when film thicknesses drop below about 25 nm. In contrast to hematite, amorphous iron(III)oxide is not photocatalytic.

Crystalline, photo-active films as thin as 10 nm, however, have been successfully fabricated via atomic layer deposition, followed by heating [13]. It will be interesting to see whether doped versions of these films prove capable of delivering higher charge collection efficiencies. Obviously, to be of practical value, a means of achieving significant light harvesting would also be required; as discussed further below, recent work by Wang and co-workers involving high-area platforms for film formation represents one possible approach [6,17].

Finally, still not well understood is why the current collection efficiency, as reflected in absorbed-photon-to-current-efficiency (APCE) measurements, is strongly wavelength dependent, varying by roughly an order of magnitude for short versus long wavelength excitation. The consequences, however, are striking: neglecting reflection losses—but assuming a 400 nm spectral cut-off due to competitive absorption by a current collector—the maximum achievable photocatalytic current density with hematite at an intensity of 1 sun and a uniform APCE of 1 would be 11.1 mA/cm^2. If light collection is extended to 300 nm (for example, by back-side illumination), the maximum possible photocurrent density would be 13 mA/cm^2. From the wavelength-dependent APCE data obtained by Wang and co-workers using hematite electrodes optimized for current collection [17], and the available solar flux at 1 sun and an AM 1.5 spectrum, we calculate maximum photocurrent densities amounting to only about one-fifth the magnitude of those anticipated based on quantitative current collection (1.8 and 2.8 mA/cm^2, respectively, for 400 and 300 nm spectral cut-offs). Clearly, if other preparative routes yield larger APCE values, the hypothetically achievable maxima, under conditions of 100% light-harvesting efficiency (LHE) for $\lambda < 610$ nm, will be higher. Nevertheless, it is notable that the best experimental systems have already reached the maxima in photocurrent density predicted based on Wang's APCE data. Thus, sizable further increases in photocurrent density in experimental systems are likely to be obtained mainly by improving charge collection (diminishing charge recombination), with further improvements in LHE yielding only modest increases.

Beside the difference in energy, the most obvious difference for hematite between photons of wavelength 300 nm versus 600 nm is that the former place photo-generated holes on bridging oxygen atoms, while the latter place them on iron atoms. For the metal-centered excitation (d–d-like excitation), subsequent spatial separation of electrons and holes presumably will create atoms having partial Fe(II) and Fe(IV) character, respectively. The extent of departure from Fe(III) (and toward Fe(II) and Fe(IV)) should depend on the number of iron centers, respectively, over which the separated electron and hole each delocalize. It is conceivable that the mobility of high-energy holes (LMCT-derived) is greater than for low-energy ones, as the details of the transport mechanisms (involving oxygen p orbitals versus iron d orbitals) clearly must be different. Higher mobility would translate into greater distances for charge separation and, presumably, smaller rates of charge recombination. In order for these differences to contribute to the observed excitation-wavelength-dependence of current collection, it would be necessary for hole transport to compete successfully with the rate of intersystem crossing from an LMCT-like excited state to a solely metal-centered (d–d) excited state.

Ultimately, for interfacial oxidation of water or hydroxide ions to be initiated, a hole must be transferred to surface adsorbed or coordinated reactants. The activation energy for this process—and, therefore, the rate—should depend strongly on whether the source of the hole is an iron center or a lattice oxygen atom. The latter presumably would be much more effective as a hole donor and perhaps less susceptible to misdirection toward unproductive recombination with an electron.

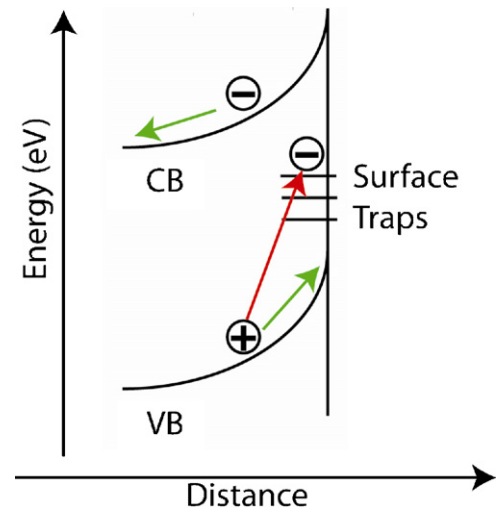

Fig. 7. Photo-generated electron/hole pair within hematite. A fraction of the holes migrating toward the photoelectrode surface recombine with electrons that are trapped in surface defect states. Atomic layer deposition of alumina is effective for pacifying (eliminating) the surface electronic states, leaving more holes free to participate in water oxidation.

3.4. Slowing surface recombination of holes and electrons

Photo-generated holes that successfully navigate the interior of a hematite electrode and reach the electrode/solution interface are still susceptible to loss via recombination with electrons; Fig. 7. Compelling evidence that recombination (at least, in part) is mediated by surface defect states comes from studies of the effects of ALD of electronically innocent metal oxides alumina on hematite photo-electrode surfaces [47]. (While alumina is unstable to dissolution in highly basic solutions, deposited material can persist long enough for photo-electrochemical measurements to be done.) Observed with ALD-alumina-modified hematite are shifts of up to −100 mV the onset potential for photocurrent production, but little change in the maximum photocurrent density [47]. Presumably the role of alumina is to provide surface iron atoms with the full complement of oxo ligands, thereby eliminating electronically discrete, mid-gap states associated with incompletely or "incorrectly" coordinated atoms. In any case, work by Hamann, Bisquert, and their co-workers has convincingly established via capacitance measurements the population and energy of surface defect sites (trap sites) that catalyze electron/hole recombination, and confirmed that they can be eliminated by ALD of small amounts of alumina [48]. Their work also shows that these sites engender Fermi-level pinning (at the energy of the traps themselves).

In related work, but utilizing photo-modulated current and voltage spectroscopy methods, Peter et al. have been able to measure, as a function of applied external bias, the first-order rate constants for surface-mediated charge recombination (k_r) and photo-assisted water or hydroxide oxidation (k_t) [19,20]. The relative magnitudes of these two processes determines the extent to which photo-generated holes that reach the hematite/solution interface can be used for photocurrent production and dioxygen production.

Peter's results at pH = 13.5 are summarized in Fig. 8 [20]. The key findings are as follows: (1) The rate constant for surface-mediated charge recombination (k_r) progressively increases as the potential moves less positive. (2) A significant uptick in k_r is observed around the potential identified by both Peter et al. [19,20] and by Hamann, Bisquert and co-workers [21] as corresponding to populating surface traps with electrons. (3) At far positive potentials, the rate constant for photo-catalytic oxidation of hydroxide ion or water exceeds the rate constant for recombination, but the

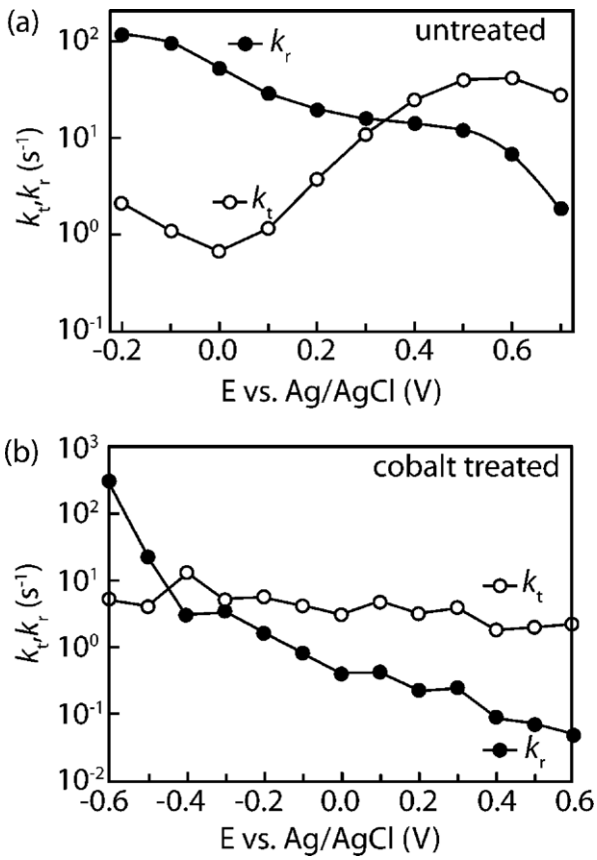

Fig. 8. Surface mediated charge-recombination rate constant (k_r), and charge-transfer constant rate (k_t) as a function of potential for (a) untreated, and (b) cobalt(II) treated hematite films.

Reprinted with permission from [20]. Copyright 2012 Royal Society of Chemistry.

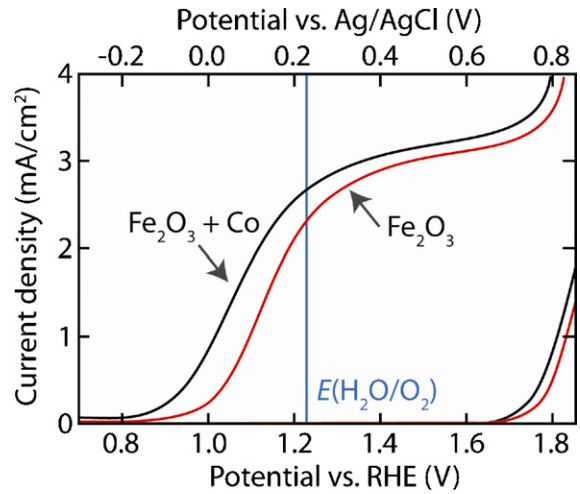

Fig. 9. Current–voltage characteristics of an unmodified (red curves) and subsequently cobalt-treated (black curves) under both dark and simulated sunlight conditions in water pH 13.6. (Note that the thermodynamic potential for water oxidation systematically shifts systematically with pH when measured against a pH-independent reference electrode such as Ag/AgCl, but is constant when measured against a reversible hydrogen electrode (RHE). The relationship between reference electrodes is $E_{RHE} = E_{Ag/AgCl} + 0.20\,V + pH \times 0.059\,V$.)

Reprinted with permission from [28]. Copyright 2006 American Chemical Society.

rate constants become equal at ~320 mV versus Ag/AgCl. These findings are consistent with the parallel observation that the photocurrent decreases significantly as the externally applied bias is decreased and approaches 320 mV. (4) Over a range of 900 mV, the rate constant for photo-catalytic oxidation of hydroxide ion or water varies only by about a factor of fifty, with the variations being non-monotonic.

Peter et al. also examined hematite electrodes that had been treated with Co^{2+}. Previous work had established that Co^{2+} exposure lowers the onset potential for photo-oxidation by roughly 80 mV (Fig. 9) [28] Given the ability of various cobalt-oxide-containing materials to catalyze the (dark) electrochemical oxidation of water or hydroxide ion to O_2, a reasonable interpretation is that adsorbed cobalt ions serve to catalyze the oxidation evolution reaction. Peter's results (summarized in Fig. 8), and earlier results from LeFormal et al., show instead that the onset potential for photocatalysis is favorably shifted because the adsorbed ions slow, by 10 to 100-fold, the rate of surface-mediated recombination of holes with electrons. In other words, cobalt ions appear to alter hematite photoelectrochemistry mainly by passivating surface defect states, in much the same fashion as alumina or gallium oxide.

Returning to Fig. 8b, the primary effect of adsorbed cobalt ions upon the rate constant for photoelectrochemical oxidation of hydroxide ions or water molecules is to render k_t even less dependent upon the applied electrode potential. The result can be contrasted with the electrochemical kinetic behavior typically seen with conductive electrodes under dark conditions, i.e. exponential increases in current density with increasing potential versus a fixed reference electrode. For metal electrodes, or electrodes having sufficient doping to mimic metal electrodes, the exponential rate versus driving force behavior can be readily understood: the thermodynamic oxidizing strength of a hole within the electrode is identical to the potential of the electrode. Increasing the electrode potential lowers the activation barrier to hole transfer from the electrode to a solution-phase reactant and yields linear free energy relationships not unlike those encountered in a wide variety of other kinetically controlled chemical processes. Thus, the log of the electrochemical rate constant increases steadily with increasing thermodynamic driving force (i.e. free-energy of the hole as defined by the electrode potential). The slopes of these plots—or, equivalently, the slopes of plots of log J versus electrode potential (Tafel plots)—contain important mechanistic information and, thus, are often collected for kinetically controlled, dark electrochemical processes.

It is important to understand that, with regard to the effects of externally applied potential, the behavior of photo-generated oxidizing equivalents (holes) within semiconducting materials like hematite is fundamentally different than the behavior of holes within highly conductive dark electrodes. For a well-behaved semiconductor-based electrode, the valence- and conduction-band-edge energies are unchanged by application of an external electrical bias. Instead what changes is the Fermi level of the semiconductor and therefore the degree of band-bending. If we avoid the special case where the applied electrode potential is positive of the valence band-edge energy, if defect states are unimportant, and if holes must reach the semiconductor/solution interface before they can be deployed for oxidation (i.e. hole tunneling from within the electrode to a solution-phase reactant is negligible), the oxidizing strength of the hole is determined by the valence-band-edge energy. Consequently, apart from minor effects such as potential-dependent adsorption or orientation of molecular reactants at the electrode surface, we expect the rate constant for transfer of photo-generated holes to molecular reactants to be insensitive to the applied potential [4].

The work of Peter et al., especially as summarized in Fig. 8, is of exceptional mechanistic importance [19,20]; it shows that for photoelectrochemical oxidation of water molecules or hydroxide ions, hematite behaves in essentially textbook fashion. The

work of Hamann, Bisquert, and co-workers offers important insight into how the story becomes more complex when surface-localized electron trap states are plentiful enough to engender Fermi-level pinning [48]. Additionally, both studies, as well as transient absorption studies by Durrant and co-workers [22], illustrate just how slowly photo-generated holes are transferred from hematite to water or hydroxide ions. Indeed, potential-insensitive reaction half-lives are on the order of a few seconds. The observed slow kinetics clearly derives from the inherent complexity of the oxygen evolution reaction. As one would anticipate, when water and hydroxide ions are replaced by hydrogen peroxide [49] (a mechanistically less demanding and thermodynamically more favorable oxidation target) or by simple, one-electron outer-sphere reactants [13], hole transfer becomes much more rapid.

3.5. Enhancing conductivity

Based on several studies, doping hematite with between roughly 1 and 10% Ti(IV), Si(IV), or Sn(IV) can substantially increase photocurrents (with further doping generally being less effective) [6,24,50,51]. By introducing additional majority carriers, doping clearly boosts hematite's conductivity and this is the effect most often cited to account for the enhancements. An attractive alternative or additional explanation is that doping aids in charge separation (diminishes bulk recombination) by bending bands more sharply, as discussed in Section 3.

A rather remarkable feature of electronic conductivity within hematite is its anisotropy—three to four orders of magnitude greater along the (0 0 1) basal plane, than perpendicular to it [52]. As noted above, doping with Si(IV) can, under some fabrication conditions, induce hematite to grow with the basal plane (see structural illustration in Fig. 10) oriented normal to a planar current collector [28]. Thus, the material is shaped and oriented such that electron transport to or from the hematite solution interface is slow, but electron transport toward the current collector is fast.

An interesting alternative to improving hematite conductivity is to turn to ultra-thin layers where charge-transport distances are so short (a few tens of nanometers or less) that photoelectrode resistivity is inconsequential. This approach makes use of high-area distributed current collectors (for example, transparent conducting oxides) [53] to enable ample light to be collected by thin hematite coatings. Pioneered by Wang et al., this strategy has been implemented with aluminum-doped zinc oxide nanotubes and with titanium silicide "nanonets" as distributed current collectors [6,54]. The required conformal coating with hematite was achieved via atomic layer deposition of amorphous Fe_2O_3, followed by heating at 500 °C to induce crystallization. While the initial results are promising, the researchers point out that there remains considerable room for improvement. Finally, a similar approach by Sivula et al., based on comparatively high area tungsten trioxide as a current collector, should be noted [55].

3.6. Altering band-edge energies

Since the formal potentials for the water-splitting half-reactions are pH dependent, one might think that manipulating the solution pH could alter the energetics so that both half reactions—not just the oxidation reaction—are aligned suitably with the band edges of the photocatalyst. Unfortunately, the band edges for α-Fe_2O_3, as well as other metal-oxide semiconductors, move with pH in the same way as the formal potentials for the water splitting half-reactions. An alternative strategy for shifting one or both edges would be to introduce ionic dopants. In particular, transition-metal ions, if added in high enough concentration, might be expected to shift the energy of the conduction band since the band is largely derived from empty metal d-orbitals. Unfortunately, apart from one recent computational study focusing on doping with Cu^{2+} [56], there is little indication, either computationally or experimentally, that the conduction-band edge of hematite can be shifted sufficiently by typical metal-ion dopants to make the material energetically viable as a photocatalyst for water reduction. (Additionally problematic is the likelihood that doping with metal atoms in oxidation state II will covert hematite to a p-type semiconductor, i.e. a form that will tend to deliver electrons rather than holes to the photo-electrode/solution interface when irradiated.) An experimental study by Hu et al. shows that fluoride (in solution) can shift the conduction band edge far enough negative (i.e. high enough in absolute energy) to reach the thermodynamic potential for reduction of water to dihydrogen, but not far enough to allow photo-generated conduction-band electrons to drive the reduction at an appreciable rate [57].

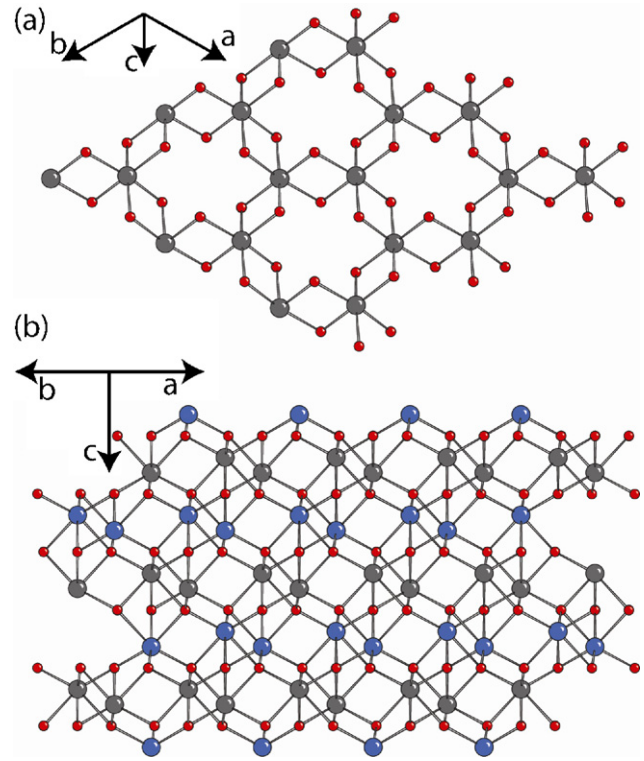

Fig. 10. crystal structure of hematite. (a) The basel plane (1 1 0) of hematite showing a layer of octahedrally coordinated iron-centers. (b) Connectivity of planes in (a). The layers stack on top of each other via the formation of face-sharing octahedra. Although crystallographically equivalent, the iron-centers of alternating planes are colored differently for clarity. Alternatively, the layers in (a) can be viewed as being linked to one another by Fe(III) sites (blue iron-centers).

3.7. Catalyzing oxygen evolution

At sufficiently high driving forces, the rate of oxygen evolution, as indicated by the plateau value of the photocurrent, is largely governed by the rate of delivery of holes to the electrode/solution interface. The delivery rate, in turn, is determined by the light intensity, the light-harvesting efficiency of the photo-electrode, and the rate of charge recombination within the electrode, relative to the kinetics of diffusion- and drift-controlled hole transport. Away from the photocurrent plateau region (i.e. at lower driving force), the rate of oxygen evolution is governed by the rate of hole transfer to H_2O or OH^-, relative to the rate of surface-mediated electron/hole recombination. Fig. 11, adapted from Valdes et al. [9], emphasizes the roles of hole delivery to the electrode surface and hole transfer to reactants in solution in determining, respectively, the limiting

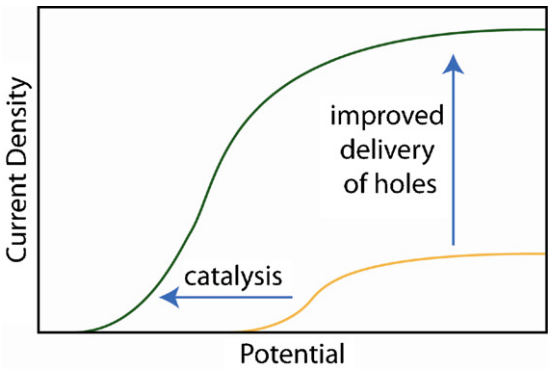

Fig. 11. Idealized J–V curves for hematite-based photo-oxidation of water. The orange curve illustrates the typical of hematite electrode. Improving the catalytic behavior of hematite would produce a photo-catalyst with earlier onset potential, while improving the delivery of holes to the hydroxide ions would increase the plateau current of the photo-electrode. The behavior of a hypothetical, optimized photo-electrode is shown in green.

photocurrent and the onset potential for photocurrent production. In this section we will mainly be concerned with the latter.

From the investigations, in particular, of Peter et al. (see Section 3.4) [19,20], it is clear that the kinetics of photoelectrochemical oxygen evolution, as gauged by the onset potential for photocurrent generation, can be improved either by lowering potential-dependent rate constants for surface-mediated charge recombination or by increasing the rate constant for hole transfer from the photo-electrode to the molecular reactant. As discussed above, the former can be accomplished by passivating surface-localized electron trap states—for example, via adsorption of Co(II) ions or via ALD of small quantities of redox-inactive materials such as alumina. The latter arguably is more challenging, as it is difficult to see how hematite itself could be induced to transfer photo-generated holes more rapidly.

An alternative approach would be to coat or attach to α-Fe_2O_3 a material or molecule capable of transferring holes to H_2O or OH^- much more quickly. For details about accelerating hole transfer, the literature on electrochemical catalysis of oxygen evolution should be consulted [58–60]. Briefly, however, effective electrochemical catalysts typically function by coupling hole transfer to proton transfer in ways that avoid high-energy intermediates and by appropriately optimizing the strengths of binding or adsorption of reactants, intermediates, and product (O_2) to molecule- or materials-based catalysts.

Work by Tilley et al., involving the attachment of iridium oxide nanoparticles to hematite photo-electrodes, is perhaps the best example of the above approach [61]. Ir_2O_3 particle attachment reduces by 200 mV the onset potential for photocurrent production by hematite. The results are impressive and represent the most favorable photocurrent onset potentials reported to date for hematite-based oxygen evolution. At the same time, in view of the remarkable catalytic activity of iridium oxide for oxygen evolution, it is surprising that the observed onset potential still exceeds by several hundred millivolts the minimum onset potential theoretically achievable. In order to convert photonic energy to stored chemical energy efficiently, it is important that water-splitting schemes operate with minimal overpotential.

The available results with iridium oxide [60] suggest that hole transfer from hematite to the catalyst might constitute a kinetic bottleneck. One approach to investigating this question would be to replace nanoparticles with porous iridium oxide films of the sort described recently by Brudvig, Crabtree, and co-workers [62]. They observed in electrochemical studies with dark electrodes, that as iridium-oxide films were made thicker, the films yielded progressively larger catalytic currents at a given potential—or, equivalently, required progressively smaller overpotentials at a given catalytic current density. These findings are consistent with involvement of sites throughout the films, and not just on the film exterior, in the oxygen evolution reaction. Extending this work to hematite photo-electrodes, one would expect photocurrent onset potentials likewise to decrease with increasing catalyst film thickness, if hole transfer from hematite to iridium oxide is rapid in comparison to subsequent transfer of oxidizing equivalents from the catalytic coating to water or hydroxide. In contrast, if hole transfer from hematite to iridium oxide is slow, increasing the thickness of the catalytic film will not diminish onset potentials.

Other attractive candidates as coating-based catalysts include nickel oxide and "CoPi", a material discovered by Kanan and Nocera and comprising phosphate-linked cobalt-oxo clusters [63]. Gamelin and co-workers have shown that CoPi coatings decrease by ~100 mV the onset potential for photocurrent production by illuminated hematite [64,65]. They have attributed the effect to increases in the rate constant for transfer of photo-generated holes to molecular reactants. An alternative explanation, suggested by Barasso et al. [14], is that CoPi behaves in a manner reminiscent of, but not identical to, adsorbed Co^{2+}. In the absence of additional experiments, it is difficult to say conclusively which explanation is more correct.

4. Conclusions

Research over the past six years has yielded substantial advances in methods for hematite-based photo-electrode fabrication and in our understanding of what still limits hematite structures as catalysts for photo-electrochemical oxidation of water or hydroxide to dioxygen. While sizable improvements in both photocurrent densities and onset potentials have been achieved in rational fashion via a variety of clever schemes, substantial further improvements in both are needed in order for hematite to become useful as a photocatalyst for water oxidation. Arguably key to attaining vast improvements in absolute rates of water oxidation and, therefore, sizable negative shifts in onset potentials, is a detailed mechanistic understanding of the hematite-facilitated pathway from water or hydroxide to dioxygen. In comparison to catalytic water oxidation pathways at dark electrodes such as ones based on iridium oxide, nickel oxide, or cobalt oxide, remarkably little mechanistic understanding exists. Also likely important will be obtaining an understanding of what controls the rate of transfer of holes from hematite to catalyst coatings, especially if this process proves to be slow in comparison to rates of hole transfer from the best catalysts to H_2O or OH^-. Whether hematite eventually becomes a practical photo-catalyst for water oxidation remains to be seen. It seems likely, however, that the schemes developed and the lessons learned in understanding and improving α-Fe_2O_3 as a photocatalyst will prove transferrable to other candidate photocatalyst materials.

Acknowledgments

We gratefully acknowledge the ANSER Center, an Energy Frontier Research Center funded by the U.S. Department of Energy, Office of Science, Office of Basic Energy Sciences under Award Number DE-SC0001059, for support of our own work on hematite and photocatalysis. The electron microscopy was accomplished at the Electron Microscopy Center for Materials Research at Argonne National Laboratory, a U.S. Department of Energy Office of Science Laboratory operated under Contract No. DE-AC02-06CH11357 by UChicago Argonne, LLC.

References

[1] M.P. Dareedwards, J.B. Goodenough, A. Hamnett, P.R. Trevellick, J. Chem. Soc. Faraday Trans. 1 (1983) 2027.
[2] K.L. Hardee, A.J. Bard, J. Electrochem. Soc. 123 (1976) 1024.
[3] J.H. Kennedy, K.W. Frese, J. Electrochem. Soc. 125 (1978) 709.
[4] M.G. Walter, E.L. Warren, J.R. McKone, S.W. Boettcher, Q. Mi, E.A. Santori, N.S. Lewis, Chem. Rev. 110 (2010) 6446.
[5] K. Sivula, F. Le Formal, M. Grätzel, ChemSusChem 4 (2011) 432.
[6] Y. Ling, G. Wang, D.A. Wheeler, J.Z. Zhang, Y. Li, Nano Lett. 11 (2011) 2119.
[7] T.W. Hamann, Dalton Trans. (2012) 7830.
[8] P.D. Tran, L.H. Wong, J. Barber, J.S.C. Loo, Energy Environ. Sci. 5 (2012) 5902.
[9] A. Valdes, J. Brillet, M. Grätzel, H. Gudmundsdottir, H.A. Hansen, H. Jonsson, P. Klupfel, G.J. Kroes, F. Le Formal, I.C. Man, R.S. Martins, J.K. Norskov, J. Rossmeisl, K. Sivula, A. Vojvodic, M. Zach, Phys. Chem. Chem. Phys. 14 (2012) 49.
[10] K. Sivula, F. Le Formal, M. Grätzel, ChemSusChem (2011) 432.
[11] J.W. Sun, D.K. Zhong, D.R. Gamelin, Energy Environ. Sci. 3 (2010) 1252.
[12] S.R. Pendlebury, M. Barroso, A.J. Cowan, K. Sivula, J. Tang, M. Grätzel, D. Klug, J.R. Durrant, Chem. Commun. 47 (2011) 716.
[13] B.M. Klahr, A.B.F. Martinson, T.W. Hamann, Langmuir 109 (2010) 13685.
[14] M. Barroso, A.J. Cowan, S.R. Pendlebury, M. Grätzel, D.R. Klug, J.R. Durrant, J. Am. Chem. Soc. 133 (2011) 14868.
[15] B.M. Klahr, T.W. Hamann, J. Phys. Chem. C 115 (2011) 8393.
[16] A.B.F. Martinson, M.J. DeVries, J.A. Libera, S.T. Christensen, J.T. Hupp, M.J. Pellin, J.W. Elam, J. Phys. Chem. C 115 (2011) 4333.
[17] Y.J. Lin, S. Zhou, S.W. Sheehan, D. Wang, J. Am. Chem. Soc. 133 (2011) 2398.
[18] N.J. Cherepy, D.B. Liston, J.A. Lovejoy, H.M. Deng, J.Z. Zhang, J. Phys. Chem. B 102 (1998) 770.
[19] C.Y. Cummings, F. Marken, L.M. Peter, A.A. Tahir, K.G.U. Wijayantha, Chem. Commun. 48 (2012) 2027.
[20] L.M. Peter, K.G.U. Wijayantha, A.A. Tahir, Faraday Discuss. 155 (2012) 309.
[21] B.M. Klahr, S. Gimenez, F. Fabregat-Santiago, T. Hamann, J. Bisquert, J. Am. Chem. Soc. 134 (2012) 4294.
[22] A.J. Cowan, C.J. Barnett, S.R. Pendlebury, M. Barroso, K. Sivula, M. Grätzel, J.R. Durrant, D.R. Klug, J. Am. Chem. Soc. 133 (2011) 10134.
[23] Y.X. Yongjing Lin, M.T. Mayer, Z.I. Simpson, G. McMahon, S. Zhou, D. Wang, J. Am. Chem. Soc. 134 (2012) 5508.
[24] J.A. Glasscock, P.R.F. Barnes, I.C. Plumb, N. Savvides, J. Phys. Chem. C 111 (2007) 16477.
[25] R.S. Schrebler, L. Ballesteros, A. Burgos, E.C. Munoz, P. Grez, D. Leinen, F. Martin, J.R. Ramos-Barrado, E.A. Dalchiele, J. Electrochem. Soc. 158 (2011) D500.
[26] A. Duret, M. Grätzel, J. Phys. Chem. B 109 (2005) 17184.
[27] L.S. Li, Y.H. Yu, F. Meng, Y.Z. Tan, R.J. Hamers, S. Jin, Nano Lett. 12 (2012) 724.
[28] A. Kay, I. Cesar, M. Grätzel, J. Am. Chem. Soc. 128 (2006) 15714.
[29] I. Cesar, A. Kay, J.A.G. Martinez, M. Grätzel, J. Am. Chem. Soc. 128 (2006) 4582.
[30] M. Cornuz, M. Grätzel, K. Sivula, Chem. Vapor Depos. 16 (2010) 291.
[31] B.M. Klahr, T.W. Hamann, Appl. Phys. Lett. 99 (2011) 063508.
[32] P. Liao, E.A. Carter, J. Phys. Chem. C 115 (2011) 20795.
[33] P. Liao, M.C. Toroker, E.A. Carter, Nano Lett. 11 (2011) 1775.
[34] P. Kumar, P. Sharma, R. Shrivastav, S. Dass, V.R. Satsangi, Int. J. Hydrogen Energy 36 (2011) 2777.
[35] N. Pailhe, A. Wattiaux, M. Gaudon, A. Demourgues, J. Solid State Chem. 181 (2008) 2697.
[36] F.L. Souza, K.P. Lopes, P.A.P. Nascente, E.R. Leite, Sol. Energy Mater. Sol. Cells 93 (2009) 362.
[37] K.L. Kelly, E. Coronado, L.L. Zhao, G.C. Schatz, J. Phys. Chem. B 107 (2003) 668.
[38] G.C. Schatz, Acc. Chem. Res. 17 (1984) 370.
[39] S.L. Pan, L.J. Rothberg, J. Am. Chem. Soc. 127 (2005) 6087.
[40] S. Standridge, G.C. Schatz, J.T. Hupp, J. Am. Chem. Soc. 131 (2009) 8407.
[41] H. Chen, J.M. McMahon, M.A. Ratner, G.C. Schatz, J. Phys. Chem. C 114 (2010) 14384.
[42] H. Chen, M.G. Blaber, S.D. Standridge, E.J. DeMarco, J.T. Hupp, M.A. Ratner, G.C. Schatz, J. Phys. Chem. C 116 (2012) 10215.
[43] N.C. Jeong, C. Prasittichai, J.T. Hupp, Langmuir (2011) 14609.
[44] J.F. Qi, X.N. Dang, P.T. Hammond, A.M. Belcher, ACS Nano 5 (2011) 7108.
[45] I. Thomann, B.A. Pinaud, Z.B. Chen, B.M. Clemens, T.F. Jaramillo, M.L. Brongersma, Nano Lett. 11 (2011) 3440.
[46] S.C. Warren, E. Thimsen, Energy Environ. Sci. 5 (2012) 5133.
[47] F. Le Formal, N. Tétreault, M. Cornuz, T. Moehl, M. Grätzel, K. Sivula, Chem. Sci. 2 (2011) 737.
[48] S.G. Benjamin Klahr, F. Fabregat-Santiago, T. Hamann, J. Bisquert, J. Am. Chem. Soc. 132 (2012) 4294.
[49] H. Dotan, K. Sivula, M. Grätzel, A. Rothschild, S.C. Warren, Energy Environ. Sci. 4 (2011) 958.
[50] G.M. Wang, Y.C. Ling, D.A. Wheeler, K.E.N. George, K. Horsley, C. Heske, J.Z. Zhang, Y. Li, Nano Lett. 11 (2011) 3503.
[51] I. Cesar, K. Sivula, A. Kay, R. Zboril, M. Grätzel, J. Phys. Chem. C 113 (2009) 772.
[52] D. Benjelloun, J.P. Bonnet, J.P. Doumerc, J.C. Launay, M. Onillon, P. Hagenmuller, Mater. Chem. Phys. 10 (1984) 503.
[53] A.B.F. Martinson, J.W. Elam, J. Liu, M.J. Pellin, T.J. Marks, J.T. Hupp, Nano Lett. 8 (2008) 2862.
[54] H. Wang, T. Deutsch, J.A. Turner, J. Electrochem. Soc. 155 (2008) F91.
[55] K. Sivula, F. Le Formal, M. Grätzel, Chem. Mater. 21 (2009) 2862.
[56] X.Y. Meng, G.W. Qin, S. Li, X.H. Wen, Y.P. Ren, W.L. Pei, L. Zuo, Appl. Phys. Lett. 98 (2011) 112104.
[57] Y.S. Hu, A. Kleiman-Shwarsctein, G.D. Stucky, E.W. McFarland, Chem. Commun. (2009) 2652.
[58] M.E.G. Lyons, M.P. Brandon, Int. J. Electrochem. Sci. 3 (2008) 1386.
[59] J. Suntivich, K.J. May, H.A. Gasteiger, J.B. Goodenough, Y. Shao-Horn, Science 334 (2011) 1383.
[60] I.C. Man, H.Y. Su, F. Calle-Vallejo, H.A. Hansen, J.I. Martinez, N.G. Inoglu, J. Kitchin, T.F. Jaramillo, J.K. Norskov, J. Rossmeisl, ChemCatChem 3 (2011) 1159.
[61] S.D. Tilley, M. Cornuz, K. Sivula, M. Grätzel, Angew. Chem. Int. Ed. (2010) 6405.
[62] J.D. Blakemore, N.D. Schley, G.W. Olack, C.D. Incarvito, G.W. Brudvig, R.H. Crabtree, Chem. Sci. 2 (2011) 94.
[63] M.W. Kanan, D.G. Nocera, Science 321 (2008) 1072.
[64] D.K. Zhong, D.R. Gamelin, J. Am. Chem. Soc. 132 (2010) 4202.
[65] D.K. Zhong, J. Sun, H. Inumaru, D.R. Gamelin, J. Am. Chem. Soc. 131 (2009) 6086.